Received: 5 September 2023 | Revised: 28 October 2023 | Accepted: 8 November 2023

DOI: 10.1002/agt2.466

Aggregate Open Access WILEY

RESEARCH ARTICLE

Miscibility screening promotes the efficiency and stability of P3HT-based organic solar cells

Special Issue: Emerging Investigators

Kaihu Xian[1] | **Ruijie Ma**[2] | **Kangkang Zhou**[1] | **Junwei Liu**[1] | **Mengyuan Gao**[1] | **Wenchao Zhao**[3] | **Miaomiao Li**[1] | **Yanhou Geng**[1,4] | **Long Ye**[1,5]

[1]School of Materials Science and Engineering, Tianjin Key Laboratory of Molecular Optoelectronic Sciences, Collaborative Innovation Center of Chemical Science and Engineering, Tianjin University, Tianjin, China

[2]Department of Electronic and Information Engineering, Research Institute for Smart Energy (RISE), Guangdong-Hong Kong-Macao (GHM) Joint Laboratory for Photonic-Thermal-Electrical Energy Materials and Devices, The Hong Kong Polytechnic University, Kowloon, China

[3]Co-Innovation Center of Efficient Processing and Utilization of Forest Resources, College of Materials Science and Engineering, Nanjing Forestry University, Nanjing, China

[4]Joint School of National University of Singapore and Tianjin University, International Campus of Tianjin University, Fuzhou, China

[5]Hubei Longzhong Laboratory, Xiangyang, China

Correspondence
Long Ye, School of Materials Science and Engineering, Tianjin Key Laboratory of Molecular Optoelectronic Sciences, Tianjin University, Collaborative Innovation Center of Chemical Science and Engineering, Tianjin 300350, China.
Email: yelong@tju.edu.cn

Ruijie Ma, Department of Electronic and Information Engineering, Research Institute for Smart Energy (RISE), Guangdong-Hong Kong-Macao (GHM) Joint Laboratory for Photonic-Thermal-Electrical Energy Materials and Devices, The Hong Kong Polytechnic University, Hung Hom, Kowloon, Hong Kong 999077, China.
Email: ruijie.ma@polyu.edu.hk

Funding information
National Natural Science Foundation of China, Grant/Award Numbers: 52073207, 52121002; Open Fund of the Hubei Longzhong Laboratory, Grant/Award Number: 2022KF-01; Peiyang Scholar Program of Tianjin University; PolyU Distinguished Postdoctoral Fellowship, Grant/Award Number: 1-YW4C; Shanghai Synchrotron Radiation Facility; Fundamental Research Funds for the Central Universities; Beijing Synchrotron Radiation Facility

Abstract

The power conversion efficiency of organic photovoltaics (OPVs) has witnessed continuous breakthroughs in the past few years, mostly benefiting from the extensive use of a facile ternary blending strategy by blending the host polymer donor:small molecule acceptor mixture with a second small molecule acceptor. Nevertheless, this rather general strategy used in the well-known PM6 systems fails in constructing high-performance P3HT-based ternary OPVs. As a result, the efficiencies of all resulting ternary blends based on a benchmark host P3HT:ZY-4Cl and a second acceptor are no more than 8%. Employing the mutual miscibility of the binary blends as a guide to screen the second acceptor, here we were able to break the longstanding 10%-efficiency barrier of ternary OPVs based on P3HT and dual nonfullerene acceptors. With this rational approach, we identified a multifunctional small molecule acceptor BTP-2Br to simultaneously improve the photovoltaic performance in both P3HT and PM6-based ternary OPVs. Attractively, the P3HT:ZY-4Cl:BTP-2Br ternary blend exhibited a record-breaking efficiency of 11.41% for P3HT-based OPVs. This is the first-ever report that over 11% efficiency is achieved for P3HT-based ternary OPVs. Importantly, the study helps the community to rely less on trial-and-error methods for constructing ternary solar cells.

KEYWORDS
crystallization, miscibility, organic photovoltaics, phase separation, polythiophene

1 | INTRODUCTION

Organic photovoltaics (OPVs), as a green energy technology, has been widely studied due to their unique characteristics, such as light-weight,[1] flexibility,[2-6] rich and adjustable colors,[7-9] and full solution processing.[10-12] The advance of this photovoltaic technology is closely associated with the development of new materials.[13-17] In early research, polythiophene[18-21] has been the most extensively studied polymer due to its simple chemical structure, high scalability, and good charge transport ability, especially for poly(3-hexyl-thiophene) (P3HT):fullerene blends.[22-25] As the most classic donor material in the OPV field, P3HT is regarded as an ideal material for realizing the commercialization of OPV cells due to its simple synthesis, low cost, and good chemical stability.[26-29] Subsequently, the

This is an open access article under the terms of the Creative Commons Attribution License, which permits use, distribution and reproduction in any medium, provided the original work is properly cited.
© 2023 The Authors. *Aggregate* published by South China University of Technology; AIE Institute and John Wiley & Sons Australia, Ltd.

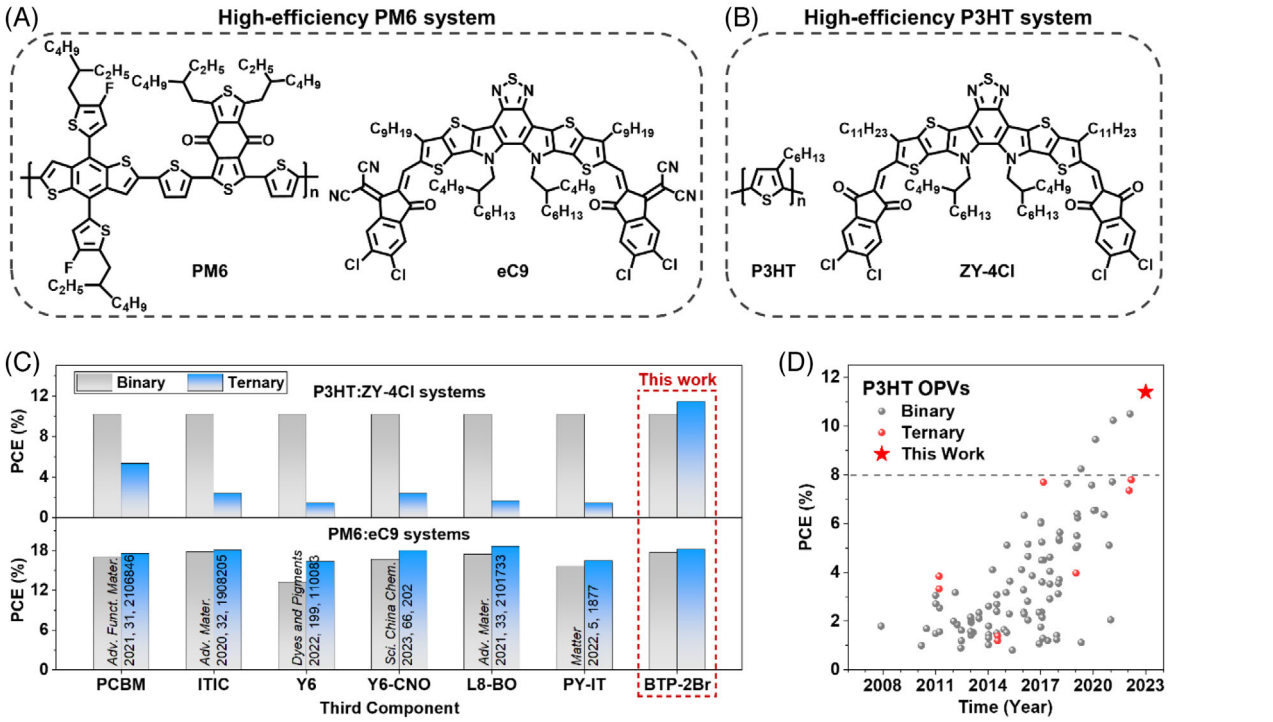

FIGURE 1 The chemical structure of the (A) well-known PM6:eC9 system and (B) P3HT:ZY-4Cl system. (C) The photovoltaic efficiency statistics of binary and ternary devices based on P3HT:ZY-4Cl and PM6:eC9 blends with various small molecule acceptors as third components. The associated references are indicated. (D) The summary of PCE records of P3HT:nonfullerene-based OPVs. The star denotes the ternary P3HT-OPVs reported in this work.

development of Y-series nonfullerene acceptors has once again improved the efficiency of low-cost systems based on polythiophenes,[30-32] which has led to the renaissance of polythiophene systems such as P3HT:nonfullerene.[33-35] Unlike the strong preaggregation nature of PM6, P3HT has insufficient phase separation with most Y-series acceptors and poor phase purity, which could be detrimental to both charge generation and transport.[36-39] Therefore, developing thermodynamically immiscible acceptors is desired for morphology optimization toward higher power conversion efficiency (PCE). In 2020, Hou and coworkers designed and synthesized a Y-series small molecule acceptor ZY-4Cl[40] with low miscibility, which achieved a record PCE of 9.46%, and it is still the only nonfullerene acceptor that delivers over 9% efficiency with P3HT. Subsequently, our group has delicately tuned the film crystallinity by substantially shortening the annealing time. As a result, the photovoltaic efficiency of P3HT:ZY-4Cl-based devices was boosted up to >10.5%.[41]

Various methods have been proposed to further improve photovoltaic efficiency and stability of P3HT-based devices.[42] Wherein ternary blending strategy has emerged as an efficacious optimization approach for OPVs and garnered significant attention over the past few years, owing to its simple device manufacturing process.[43-48] Especially, the incorporation of a second acceptor into binary systems is simple and has exhibited great potential in upgrading the photovoltaic performance of OPV for practical applications.[49-51] However, the screening of the second acceptor in ternary systems, in addition to matching energy levels and complementary absorption, is still based on trial-and-error methods.[52-54] Especially with the emergence of high-efficiency systems, the material structures and device optimization protocols have become more complex, severely limiting the applicability of the ternary blend strategy across different material systems. Taking the high-efficiency PM6:eC9 system (Figure 1A) as an example, various electron acceptors have been successfully used as third components to promote the efficiency of this benchmark system[55-59] (Table S1). However, when we further introduce these acceptor materials into another benchmark P3HT:ZY-4Cl blend (Figure 1B), all of the resulting ternary systems surprisingly achieve significantly reduced performance (Figure 1C) after incorporating the acceptors mentioned above as third components (Table S2). These sharply different roles of the same third components in P3HT and PM6 motivated us to identify a versatile acceptor to promote the efficiencies of both systems. As far as we know, none of the P3HT-based ternary OPVs reported so far can realize over 8% efficiency.[60] Moreover, the previous study based on P3HT:nonfullerene ternary system mainly focused on the classical P3HT:O-IDTBR blends,[61] while the study of P3HT ternary systems based on star Y-series acceptors is rare. Therefore, it is imperative to screen a new third component suitable for the organic photovoltaic systems through rational avenues.

In this work, we put forward a multifunctional small molecule acceptor named BTP-2Br as a third component in realizing improved performance for P3HT-based ternary OPVs, with the rational guidance of miscibility screening. It is the only acceptor to date that can concurrently improve the photovoltaic efficiencies of both P3HT:ZY-4Cl and PM6:eC9 systems (Figure 1C). Attractively, the photovoltaic efficiency of the ternary blend based on P3HT:ZY-4Cl:BTP-2Br has reached 11.41%, which is a new world record for P3HT-based OPVs (Figure 1D). By conducting a set of light source-based X-ray scattering and microscopy characterizations, we find that the introduction of BTP-2Br helps to optimize phase separation and crystallization behaviors, achieve effective exciton dissociation, balance charge

26924560, 2024, 2, Downloaded from https://onlinelibrary.wiley.com/doi/10.1002/agt2.466 by Hong Kong Poly University, Wiley Online Library on [22/04/2024]. See the Terms and Conditions (https://onlinelibrary.wiley.com/terms-and-conditions) on Wiley Online Library for rules of use; OA articles are governed by the applicable Creative Commons License

transport, and suppress recombination losses. Our miscibility analysis points out that the Flory-Huggins interaction parameter (χ)[62] between the donor and the second acceptor should be smaller than that of control binary blends. This facile strategy of miscibility screening was proposed for the first time for selecting the second acceptors suitable for multiple ternary systems. Accordingly, the P3HT-based ternary blend system exhibits a longer operational lifetime and over 11% efficiency, which outperforms all of the previously reported P3HT cells. This study firmly demonstrates the critical functions of mutual molecular interactions in regulating blend morphology and rely less on trial-and-error methods for the fabrication of high-performance ternary solar cells.

2 | RESULTS AND DISCUSSION

According to a previous study,[41] ZY-4Cl is a nonfullerene with strong self-aggregation properties, which results in excessive phase separation of P3HT:ZY-4Cl blend films upon thermal annealing. To address this issue, molecular aggregation and crystallization can be regulated through postprocessing or the introduction of solid additives[63] to suppress the strong phase separation. Additionally, weaker phase separation can be achieved through the introduction of a second acceptor, which may further improve the photovoltaic performance of the device by optimizing the light-utilization ability and energy level alignment. Miscibility[64] can be described with the material-specific Flory-Huggins interaction parameter (χ).[65] The χ parameter is ubiquitous in the description of the thermodynamics of mixtures and can be experimentally determined by many techniques.[66] The experimental determination of χ via traditional differential scanning calorimetry (DSC) methods is material consumptive. Moreover, the inability of DSC analysis to observe pronounced thermal transitions (Figure S1), our understanding of the mixing thermodynamics exhibited by these Y-series acceptors is limited. Instead, the χ value can be calculated from the Hansen solubility parameters (HSPs) of donors and acceptors. The HSPs can be estimated from functional group additive methods. The detailed HSPs of donors and acceptors used in this work are listed in Table S3.

As shown in Table S4, we first evaluated the χ of multiple commonly used acceptors and P3HT to describe the molecular interaction between P3HT and various acceptor molecules. We note that all the χ values are between 4 and 6. A high value indicates excessive phase separation between the donor and acceptor, which is not conducive to charge separation and transport in the devices. Interestingly, we find the χ parameters of most P3HT:acceptor blends are higher than that of P3HT:ZY-4Cl, as shown in Figure 2A. The higher χ values between these acceptors and P3HT will lead to the more excessive phase separation in their corresponding binary blends. Therefore, introducing a second acceptor with a smaller χ value is most likely beneficial to the device performance. To our surprise, only a brominated Y-series nonfullerene acceptor BTP-2Br proposed herein possesses a smaller χ value with P3HT than that of ZY-4Cl. Based on our calculations, the introduction of those acceptors other than BTP-2Br is not beneficial to the performance of ternary systems due to the unfavorable phase separation. In contrast, introducing BTP-2Br into the P3HT:ZY-4Cl binary control system is expected to offer better photovoltaic performance.

Motivated by this finding, we prepared the Y-series derivative BTP-2Br to verify our hypothesis. Specifically, a commercially available dithienothiopheno[3,2-*b*]-pyrrolobenzothiadiazole core was reacted with 5-bromo-1H-indene-1,3(2H)-dione by Knoevenagel condensation at 70°C for 7 days to afford dark solid target compound with a yield of 67% (see Figure 2B). The synthetic details and relevant data can be found in the Supporting Information. The electrochemical characteristic of BTP-2Br was investigated through cyclic voltammetry (CV), as illustrated in Figure S2. It can be estimated from the plots that the HOMO and LUMO levels of BTP-2Br are determined to be −5.58 and −3.63 eV, respectively. The optical property of BTP-2Br also was characterized by UV-vis absorption spectroscopy, as shown in Figure 3A, which exhibited a complementary absorption band with those of PM6:eC9 and P3HT:ZY-4Cl blends.

Having confirmed the complementary absorption and matched energy levels (Figure 3B) between BTP-2Br and P3HT:ZY-4Cl blend systems, we measured the photovoltaic properties with a conventional device structure consisting of ITO glass/PEDOT:PSS/ active layer/PDINN/Ag. The

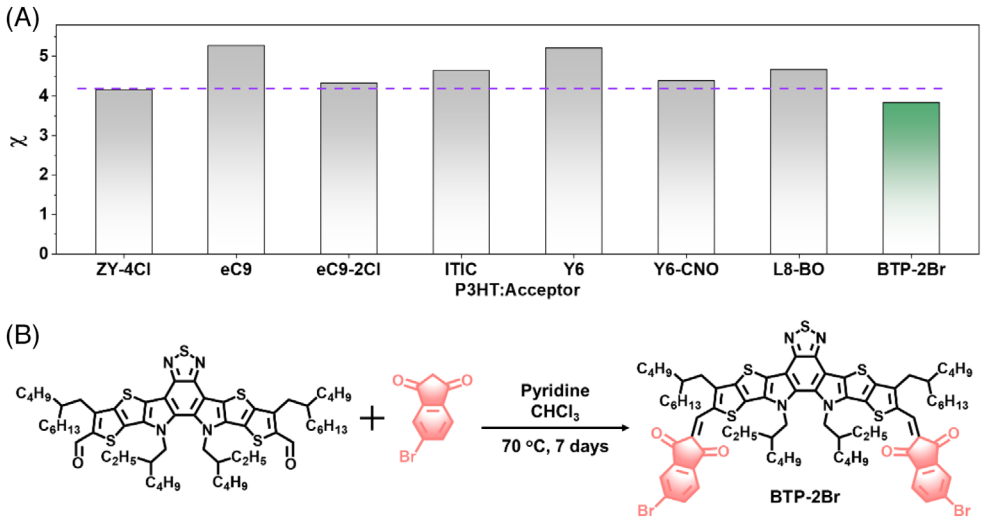

FIGURE 2 (A) The statistics of χ values between P3HT and various NFAs. (B) The synthetic route of BTP-2Br.

26924560, 2024, 2, Downloaded from https://onlinelibrary.wiley.com/doi/10.1002/agt2.466 by Hong Kong Poly University, Wiley Online Library on [22/04/2024]. See the Terms and Conditions (https://onlinelibrary.wiley.com/terms-and-conditions) on Wiley Online Library for rules of use; OA articles are governed by the applicable Creative Commons License

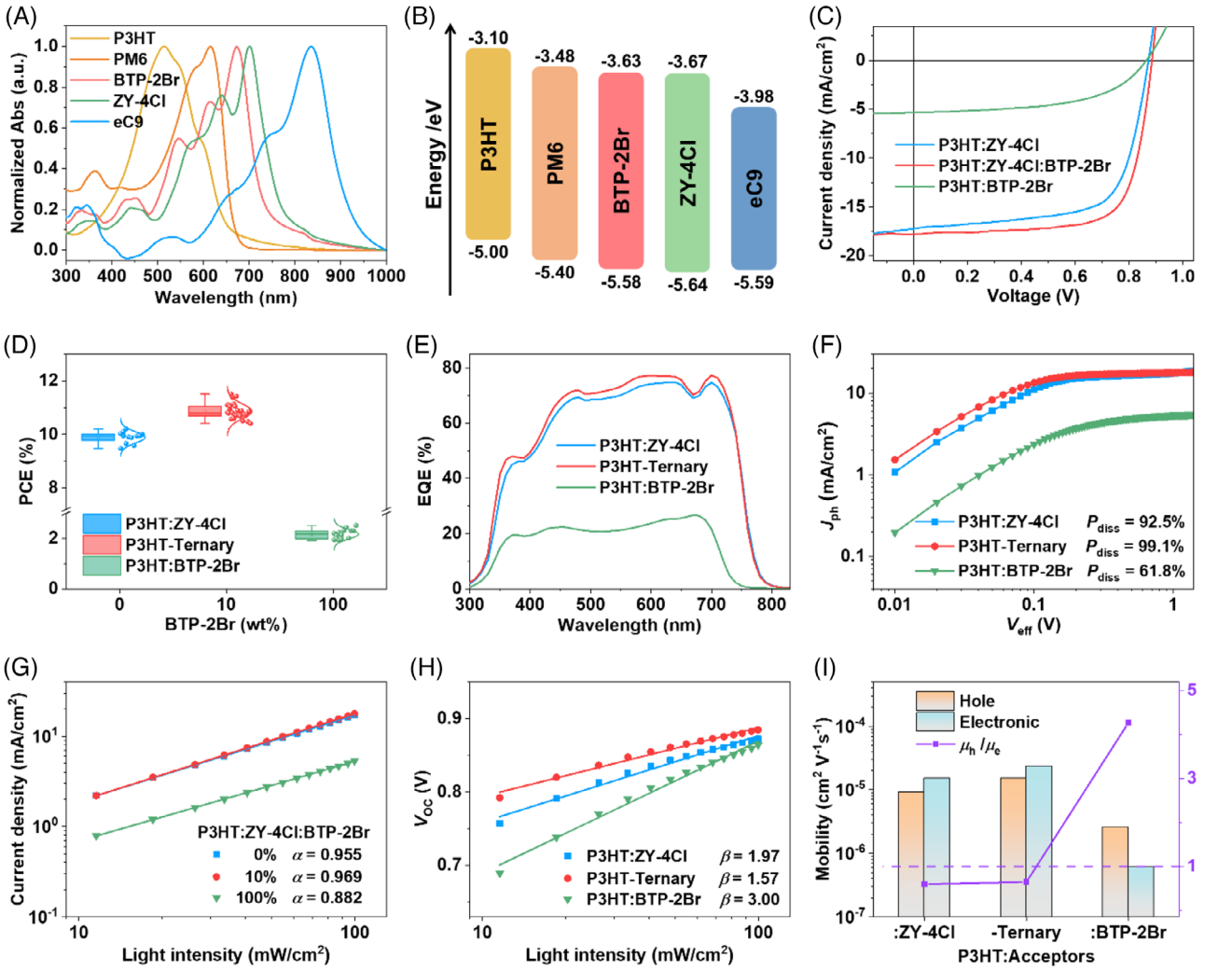

FIGURE 3 (A) Normalized absorption spectra of P3HT, PM6, BTP-2Br, ZY-4Cl, and eC9 neat films. (B) Energy level diagram of the donors and acceptors. (C) *J-V* characteristic curves of optimal devices based on P3HT:ZY-4Cl, P3HT:BTP-2Br, and P3HT:ZY-4Cl:BTP-2Br blends. (D) The PCE statistics of 12 cells for each blend. (E) The corresponding EQE curves of relevant devices. (F) J_{ph} versus V_{eff} plots of the three devices. The extracted plots of (G) J_{SC} and (H) V_{OC} versus light intensity for the P3HT-based devices. (I) The histograms of hole and electron mobilities of P3HT:ZY-4Cl, P3HT:BTP-2Br, and P3HT:ZY-4Cl:BTP-2Br blends measured by SCLC method.

TABLE 1 Photovoltaic parameters of P3HT-based OPV devices.

Active layers	V_{OC} (V)	J_{SC}[a] (mA/cm^2)	J_{cal} (mA/cm^2)	FF (%)	PCE (%)[b]
P3HT:ZY-4Cl	0.872	17.22	16.49	67.9	10.20 (9.96 ± 0.14)
P3HT:BTP-2Br	0.864	5.33	4.93	54.7	2.52 (2.26 ± 0.15)
P3HT:ZY-4Cl:BTP-2Br	0.885	17.78	17.06	72.5	11.41 (11.16 ± 0.21)

[a] J_{cal} was calculated by the EQE curve.
[b] The average values and standard deviations were obtained from 10 devices.

current density-voltage (*J-V*) curves of the optimal P3HT:ZY-4Cl:BTP-2Br blends are depicted in Figure 3C and the relevant photovoltaic parameters are summarized in Table 1 and Figure 3D. The control P3HT:ZY-4Cl-based device exhibits a PCE of 10.20%, with an open-circuit voltage (V_{OC}) of 0.872 V, a short-circuit current density (J_{SC}) of 17.22 mA/cm^2 and a fill factor (FF) of 67.9%. For the P3HT:BTP-2Br blend, a poor J_{SC} of 5.33 mA/cm^2 is obtained, accompanied by a V_{OC} of 0.864 V and a FF of 54.7%, which lead to a significantly low PCE of 2.52%. Encouragingly, after introducing a small amount (10%) of the guest acceptor into P3HT:ZY-4Cl control blend, P3HT:ZY-4Cl:BTP-2Br ternary cells received a boosted J_{SC} of 17.78 mA/cm^2 and an elevated FF of 72.5% with a V_{OC} of 0.885 V, resulting in a significantly improved champion PCE of 11.41%, which is a new record PCE for P3HT-based OPVs.

The corresponding external quantum efficiency (EQE) curves of the three optimized P3HT-based devices are displayed Figure 3E. The integrated current density values (J_{cal}) from the EQE curves are 16.49, 4.93, and 17.06 mA/cm^2 for OPVs based on P3HT:ZY-4Cl, P3HT:BTP-2Br, and P3HT:ZY-4Cl:BTP-2Br blends, respectively, which are close to those derived from the *J-V* curves. Notably, the ternary system demonstrated the highest EQE response of over 70% within the wavelength range of 450–750 nm, indicating

26924560, 2024, 2, Downloaded from https://onlinelibrary.wiley.com/doi/10.1002/agt2.466 by Hong Kong Poly University, Wiley Online Library on [22/04/2024]. See the Terms and Conditions (https://onlinelibrary.wiley.com/terms-and-conditions) on Wiley Online Library for rules of use; OA articles are governed by the applicable Creative Commons License

the quite efficient photoelectric conversion in this ternary system.

To gain a deeper understanding of the photoelectric conversion process, the relationship between photocurrent density (J_{ph}) and effective voltage (V_{eff}) of the devices was studied (as depicted in Figure 3F) to explore the charge separation and collection behaviors of the devices. J_{ph} is the difference between the current density in the dark and under illumination, V_{eff} is the difference between the voltage when J_{ph} is zero and the applied voltage. The ternary system possessed the top exciton dissociation probability (P_{diss}) value of 99.1%, which was higher than the two binary systems (92.5% for P3HT:ZY-4Cl and 61.8% for the P3HT:BTP-2Br blend). The P_{diss} is defined as the ratio of J_{SC} / J_{sat} (J_{sat} is the saturatio current density). The ternary system also displayed the highest exciton collection probability (P_{coll}) value of 87.1% among all systems (Table S5), where P_{coll} is defined as the ratio of J_{max} / J_{sat} (J_{max} is the current density under maximum power output conditions). The J_{ph} of P3HT:BTP-2Br-based devices approaches saturated at much higher V_{eff} values exceeding 2 V, indicating a lower exciton dissociation probability and diminished charge collection efficiency.

Furthermore, we measured the *J-V* curves of the devices under different light intensity to explore the charge recombination behavior in the active layer. The correlation between J_{SC} and P_{light} can be expressed as $J_{SC} \propto P_{light}^{\alpha}$, *a*s shown in Figure 3. The slope (as reflected in α values) of J_{SC} versus light intensity (P_{light}) approaching 1 indicates that the bimolecular recombination of the control binary and the optimal ternary blends are so weak that it can be ignored. Nevertheless, the trap-assisted recombination cannot be ignored in the system, as displayed in Figure 3H. The relation between V_{OC} and P_{light} can be expressed as $V_{OC} = \beta(kT/e)\ln(P_{light}) + c$, where k is the Boltzmann constant, T is the temperature, e is the elementary charge, c is the constant, and β is the scaling factor. From the β values (1.97 for P3HT:ZY-4Cl, 1.57 for P3HT:ZY-4Cl:BTP-2Br) derived from the P_{light} dependent V_{OC}, it is suggested that the BTP-2Br can suppress the trap-mediated monomolecular recombination in the devices. The exaggerated β value (3.00) and low α value (0.882) of the P3HT:BTP-2Br-based device indicate the strong charge recombination in the device, therefore presenting the terrible J_{SC} and FF. It is concluded that BTP-2Br can suppress the charge recombination and facilitate the charge extraction, which contributes to the high J_{SC} and FF in the ternary device.[67]

Subsequently, the charge mobility in the binary and ternary blend films was monitored based on the space-charge-limited current (SCLC) model, which is one of the critical factors for J_{SC} and FF. The curves of the hole- or electron-only devices are shown in Figure S3, and the relevant parameters are listed in Table S6. The calculated hole mobility (μ_h) and electron mobility (μ_e) in the active layers are plotted in Figure 3I. The μ_h and μ_e of the ternary blend were slightly improved (1.51×10^{-5}/2.34×10^{-5} cm^2 V^{-1} s^{-1}) compared with the control binary blend (9.08×10^{-6}/1.51×10^{-5} cm^2 V^{-1} s^{-1}). Normally, the degree of balance in charge carrier transport can be evaluated with the ratio of hole and electron mobility (μ_h/μ_e).[68] The μ_h/μ_e values are 0.60, 4.27, and 0.65 for devices with P3HT:ZY-4Cl, P3HT:BTP-2Br and P3HT:ZY-4Cl:BTP-2Br as active layers, respectively. The μ_h/μ_e of the optimal ternary devices is the closest to 1, indicating that adding an appropriate amount of BTP-2Br can make the charge transport more balanced in active layers. Thus, greater and more balanced charge mobilities contribute to the higher J_{SC} and FF for the optimal ternary devices.

Next, the surface morphology of the photoactive layers was monitored by atomic force microscopy (AFM). As presented in Figure 4A, the P3HT:ZY-4Cl:BTP-2Br ternary blend film exhibits a significantly reduced root-mean-square surface roughness (R_q) of 1.4 nm compared with the control binary films (1.9 nm). The P3HT:BTP-2Br blend film exhibits the smallest R_q of 0.9 nm, implying a poor phase separation in the binary film. Insufficient phase separation results in poor phase purity and smaller domains, which could be detrimental to both charge generation and transport. Furthermore, the power spectral density profiles[69] were obtained to attain the size scale of phase separation by fast Fourier transform of AFM phase images (Figure S4). As shown in Figure 4B, the characteristic length scale of the blend films gradually decreases from 56 to 50 nm, to 37 nm as the content of BTP-2Br increases, which agrees well with its smaller χ with P3HT.

In order to reveal how the addition of BTP-2Br impacts the molecular stacking of the blend films, we conducted grazing incidence wide-angle X-ray scattering (GIWAXS) measurements. The 2D scattering patterns of P3HT:ZY-4Cl, P3HT:BTP-2Br and P3HT:ZY-4Cl:BTP-2Br blend films were shown in Figure 4C, and the corresponding scattering intensity curves in the out-of-plane (OOP) and in-plane (IP) directions were displayed in Figure 4D. Both P3HT:ZY-4Cl and P3HT:ZY-4Cl:BTP-2Br blend films exhibit a more predominant face-on orientation, with a pronounced (010) diffraction signal in the OOP direction at 1.64 $Å^{-1}$. An obvious (100) diffraction signal at 0.37 $Å^{-1}$ in the IP direction can be observed, which originates from the lamellar staking of P3HT. The weak (100) diffraction signals at 0.23 $Å^{-1}$ in the IP direction and 0.51, 0.62 $Å^{-1}$ in the OOP direction are the features of ZY-4Cl. The two blend films show very little difference in diffraction signals, indicating that the introduction of BTP-2Br has no significant impact on the molecular arrangement of P3HT:ZY-4Cl. Moreover, the coherence length (CL) of π-π staking increased from 16.8 Å to 17.8 Å, and the CL of lamellar staking increased from 100.5 to 111.6 Å. The detailed parameters are summarized in Table S7-S8. Therefore, we can confirm that the addition of BTP-2Br into the P3HT:ZY-4Cl blend film leads to more ordered molecular packing. In contrast, the P3HT:BTP-2Br blend exhibits the mixed face-on and edge-on orientation, with the (100) peaks at ~0.37 $Å^{-1}$ in both OOP and IP direction. The (100) diffraction signals at 0.46 and 0.61 $Å^{-1}$ in the OOP direction correspond to the alkyl-stacking direction, originating from BTP-2Br (Figure S5 and Table S9-S10). A pronounced (010) diffraction signal in the IP direction was observed at 1.48 $Å^{-1}$, corresponding to π-π distances of 4.3 Å.

To quantify and further evaluate the effects of BTP-2Br on the film crystallinity of the blends, we further performed the pole figure analysis of the (010) π-π stacking scattering peaks in OOP directions. Figure S6 displayed the pole figures (intensity × sin(ω)~ω) of (010) π-π stacking peaks of P3HT blend systems. The relative degree of crystallinity (*rDoC*)[70] is calculated by integrating the scattering intensity of the pole figure across all polar angles from 0 to 90° based on a

26924560, 2024, 2, Downloaded from https://onlinelibrary.wiley.com/doi/10.1002/agt2.466 by Hong Kong Poly University, Wiley Online Library on [22/04/2024]. See the Terms and Conditions (https://onlinelibrary.wiley.com/terms-and-conditions) on Wiley Online Library for rules of use; OA articles are governed by the applicable Creative Commons License

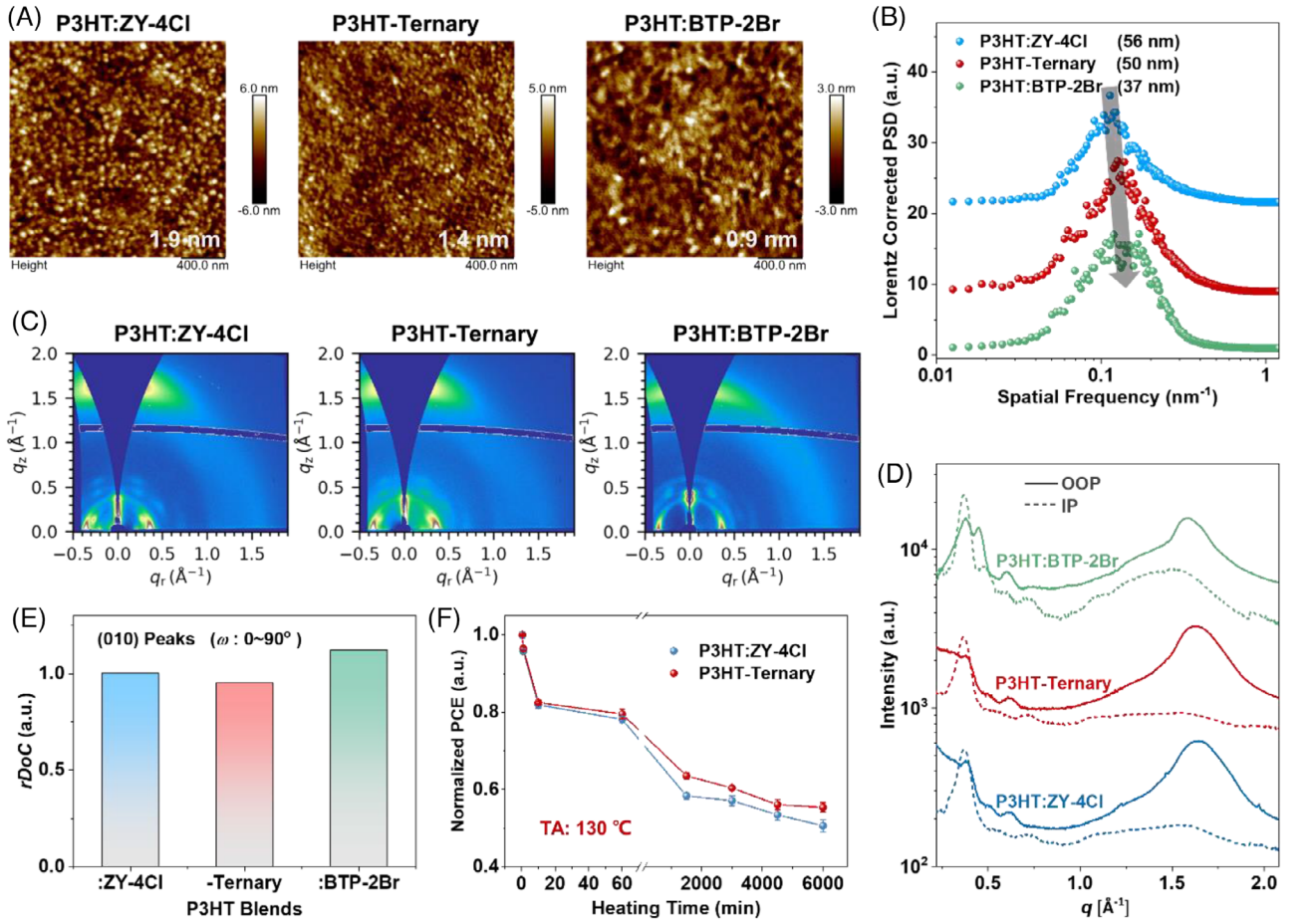

FIGURE 4 (A) The AFM height images of P3HT-based blend films. (B) Lorentz corrected power spectral density (PSD) profiles of the phase images for the three blend films. (C) The 2D GIWAXS patterns of P3HT:ZY-4Cl, P3HT:BTP-2Br and P3HT:ZY-4Cl:BTP-2Br blend films. (D) The corresponding 1D GIWAXS line profiles of the OOP and IP directions for three blend films. (E) The histogram of rDoC values calculated from the (010) peaks of the P3HT blend systems. (F) The evolution plots of normalized PCE with annealing time for the P3HT-based blend films at 130°C.

corrected Ewald sphere. The histogram of *rDoC* values of (010) peaks are shown in Figure 4E. All values are normalized to the control binary blend (P3HT:ZY-4Cl), which is assigned to be 1. The *rDoC* value of ternary blends is 0.95, suggesting a slightly suppressed crystallinity. Suppression of strong crystallization in the binary system by the introduction of BTP-2Br can suppress the formation of large crystals in the film, thereby providing a more stable film morphology, which will synergistically lead to higher device performance and thermal stability.

Thus, considering the changes in film crystallinity upon the addition of BTP-2Br, we investigated the thermal stability of the control binary and ternary blends. As shown in Figure 4F, the PCE of the control binary blend decreased to 50% of the initial efficiency after continuously annealing the blend films at 130°C for 6000 min. By comparison, the ternary blend retained a higher percentage of its initial performance, which is mostly attributed to the suppressed crystallization with smaller *rDoC* values. The results indicate that the new ternary blend possesses better thermal stability than that of the binary blends.

To test the aforementioned miscibility-guided ternary blending approach, we revisited PM6:eC9 with various acceptors. As displayed in Figure 5A, the PM6:eC9 blend possesses the maximum χ value, while the χ values of PM6 with other acceptors are all smaller than that of the control binary blend. Thus, all of these acceptors can be introduced as second acceptors to potentially improve photovoltaic efficiencies. In this regard, we introduced 10 wt% BTP-2Br into the high-efficiency system PM6:eC9, considering the lower χ value of PM6:BTP-2Br blend. As expected, the PM6:eC9:BTP-2Br-based ternary devices can obtain a higher PCE of 18.22% with a J_{SC} of 27.14 mA/cm^2, an FF of 78.2%, and a higher V_{OC} of 0.859 V, compared with the control binary cell (17.88%). The histogram of optimal devices based on PM6:eC9, PM6:BTP-2Br and PM6:eC9:BTP-2Br blends is presented in Figure 5B. The *J-V* curves and EQE curves are presented in Figure S7, respectively, and the relevant photovoltaic parameters are summarized in Table S11. It was found that the alterations in PM6 systems after introducing BTP-2Br exhibit a similar trend to the performance and stability evolutions (Figure 5C) in the above P3HT systems. The higher χ implies the stronger phase separation in the control binary blends.[62] Therefore, introducing acceptor (BTP-2Br) with lower χ value can inhibit excessive aggregation of Y-series acceptors (ZY-4Cl and eC9) and provide smaller phase separation (Figure S8), which will synergistically lead to higher device performance and thermal stability of both P3HT:ZY-4Cl systems and PM6:eC9 systems.

Subsequently, we evaluated the χ between an asymmetric acceptors Y6-CNO (see Figure 5D, an analogue of eC9 and ZY-4Cl) and the two polymers. we can find the χ parameters of P3HT:Y6-CNO blends are higher than that of P3HT:ZY-4Cl, while the χ parameters of

26924560, 2024, 2, Downloaded from https://onlinelibrary.wiley.com/doi/10.1002/agt2.466 by Hong Kong Poly University, Wiley Online Library on [22/04/2024]. See the Terms and Conditions (https://onlinelibrary.wiley.com/terms-and-conditions) on Wiley Online Library for rules of use; OA articles are governed by the applicable Creative Commons License

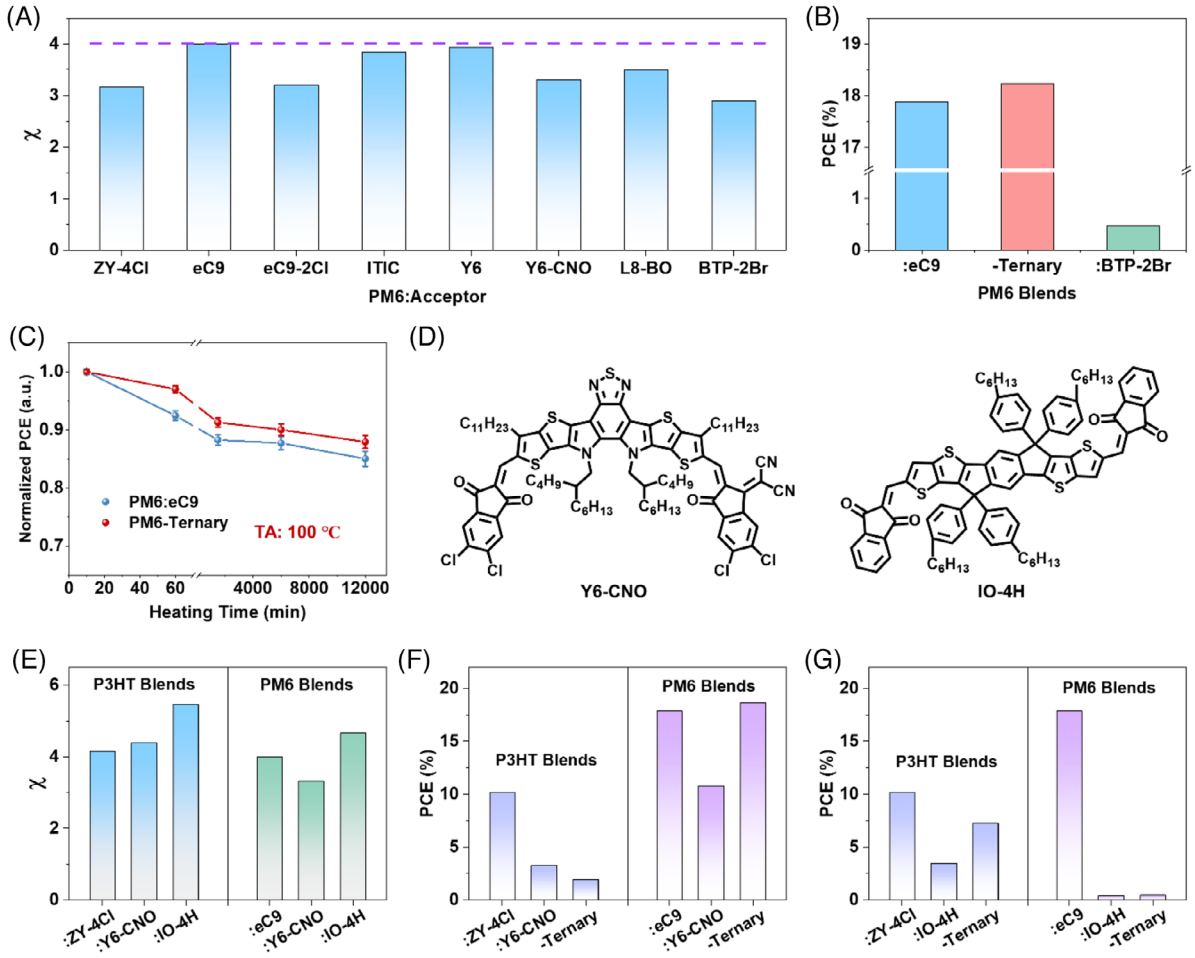

FIGURE 5 (A) The plots of χ values between PM6 and various nonfullerene acceptors. (B) The histogram of optimal devices efficiency based on PM6:eC9, PM6:BTP-2Br, and PM6:eC9:BTP-2Br blends. (C) The evolution plots of normalized PCE with annealing time for the PM6-based blend films at 100°C. (D) The chemical structure of the Y6-CNO and IO-4H. (E) The χ values of P3HT:ZY-4Cl, P3HT:Y6-CNO, P3HT:IO-4H; PM6:eC9, PM6:Y6-CNO, and PM6:IO-4H blends. (F) The histogram of optimal devices based on P3HT:ZY-4Cl, P3HT:Y6-CNO, P3HT:ZY-4Cl:Y6-CNO; PM6:eC9, PM6:Y6-CNO, and PM6:eC9:Y6-CNO blend films. (G) The histogram of efficiency based on P3HT:ZY-4Cl, P3HT:IO-4H, P3HT:ZY-4Cl:IO-4H; PM6:eC9, PM6:IO-4H, and PM6:eC9:IO-4H blend films.

PM6:Y6-CNO blends are lower than that of PM6:eC9, as shown in Figure 5E. According to our prediction, the introduction of Y6-CNO is not beneficial to the performance of P3HT-based ternary systems due to the unfavorable phase separation. In contrast, introducing Y6-CNO into the PM6:eC9 binary control system is expected to offer better photovoltaic performance. As expected, the P3HT:ZY-4Cl:Y6-CNO-based ternary devices offer a poor PCE of 1.95% by incorporating 10 wt% Y6-CNO, much lower than that of the control binary cell (10.20%). While the PM6:eC9:Y6-CNO-based ternary devices give a higher PCE of 18.66%, higher than the PCE of PM6:eC9 blends (17.88%). The histogram of optimal devices is presented in Figure 5F. The *J*-*V* curves are presented in Figure S9, and the relevant photovoltaic parameters are summarized in Table S12. ZY-4Cl is a derivative of eC9, which replaced the strong electronegative malononitrile with carbonyl group. In a similar manner, we evaluated the χ between IO-4H[71] (a derivative of ITIC, where the malononitrile in ITIC was replaced with carbonyl) and the two polymers to confirm the impact of terminal groups on performance. We found that the P3HT:IO-4H blend provides a considerably higher PCE of 3.44% than that of P3HT:ITIC (0.02%). Unfortunately, the χ values of IO-4H-based binary blends are higher than that of P3HT:ZY-4Cl and PM6:eC9, respectively. Hence, when introducing 10 wt% IO-4H into the host system, the IO-4H-based ternary devices exhibit significantly lower PCEs (7.27% for P3HT systems and 0.47% for PM6 systems) compared to the control binary devices, as shown in Figure 5. Therefore, the screening of second acceptors in ternary systems necessitates not only matching energy levels and complementary absorption but also requires further prediction of intermolecular interactions through miscibility analysis. As such, our screening strategy holds significant value in reducing reliance on trial-and-error methods for constructing high-efficiency ternary solar cells.

In ternary blend systems, there are intermolecular interactions between the donor/acceptor molecules, and mutual interactions between the donor and acceptor molecules all matter.[72] As the χ values between the nonfullerene acceptor molecules are all lower than 0.4 (Figure S10), the two acceptors are highly miscible compared with the blend between donor and acceptor molecules. Therefore, it is more important to match the miscibility between donor and acceptor. One can infer the mutual interactions in ternary blends based on the χ values of the various binary blends. Finally, a guiding principle for selecting the second acceptor for Y-series systems with strong self-aggregation characteristics emerges

26924560, 2024, 2, Downloaded from https://onlinelibrary.wiley.com/doi/10.1002/agt2.466 by Hong Kong Poly University, Wiley Online Library on [22/04/2024]. See the Terms and Conditions (https://onlinelibrary.wiley.com/terms-and-conditions) on Wiley Online Library for rules of use; OA articles are governed by the applicable Creative Commons License

as follows: the third component exhibits a χ value with the host polymer smaller than that of the host acceptor materials. The introduction of an appropriate amount of BTP-2Br can improves the photovoltaic performance and thermal stability of both P3HT:ZY-4Cl and PM6:eC9-based devices, which is well captured by our miscibility-function relations. Overall, the theoretical calculation of χ values can offer a facile guide for the selection of the third component in developing high-performance ternary OPVs, which can greatly reduce the experimental trial and error costs.[73]

3 | CONCLUSION

Motivated by theoretical calculations of blend miscibility, we designed and synthesized a versatile nonfullerene acceptor BTP-2Br as a third component to simultaneously optimize the photovoltaic performance of P3HT and PM6-based binary OPVs. Strikingly, a champion photovoltaic efficiency of 11.41% was achieved by introducing 10 wt% BTP-2Br into the P3HT:ZY-4Cl system, which was higher than that of the control binary cell (10.20%). The champion PCE attained in this work is the topmost value reported so far for P3HT-based OPVs. This study fills the existing gap in constructing high-efficiency ternary OPVs based on P3HT and nonfullerene acceptors. Moreover, a facile strategy of miscibility screening was proposed for the first time for selecting the second acceptors suitable for both P3HT and PM6-based ternary systems. With the assistance of this approach, the PM6:eC9:BTP-2Br-based ternary devices delivered a photovoltaic efficiency of 18.23%, higher than that of the control binary cell. The effectiveness of this approach is further validated with a ITIC analogue. Our study points out that the χ value between the second acceptor and the host polymer donor should be smaller than those of control binary blends. This simple approach offers great potential, as it can facilitate the selection of an optimal ternary combination with desired morphology for fabricating efficient and cost-effective optoelectronic devices. Moving forward, developing stretchable polythiophene solar cells[74,75] is of cruical importance.

ACKNOWLEDGMENTS

This research was made possible, thanks to the financial support of the National Natural Science Foundation of China (grant numbers: 52073207 and 52121002) and the Fundamental Research Funds for the Central Universities. L.Y. also appreciates the Open Fund of the Hubei Longzhong Laboratory (grant number: 2022KF-01) and the Peiyang scholar program of Tianjin University for support. GIWAXS data acquisition was carried out at the beamline 1W1A of Beijing Synchrotron Radiation Facility (BSRF). R.M. thanks the support from the PolyU distinguished Postdoctoral Fellowship (grant number: 1-YW4C). This work was also carried out with the support of Shanghai Synchrotron Radiation Facility, BL02U2. Dr. Cenqi Yan is acknowledged for the help upon material preparation.

FUNDING INFORMATION

National Natural Science Foundation of China, Grant Numbers: 52073207 and 52121002; Fundamental Research Funds for the Central Universities; Open Fund of the Hubei Longzhong Laboratory, Grant Number: 2022KF-01; Peiyang Scholar Program of Tianjin University; PolyU Distinguished Postdoctoral Fellowship, Grant Number: 1-YW4C; Beamline BL02U2 of Shanghai Synchrotron Radiation Facility; Beamline 1W1A of Beijing Synchrotron Radiation Facility.

CONFLICT OF INTEREST STATEMENT

The authors declare no conflict of interests.

DATA AVAILABILITY STATEMENT

The data that support the findings of this study are available upon request to the corresponding authors.

ORCID

Ruijie Ma https://orcid.org/0000-0002-7227-5164
Long Ye https://orcid.org/0000-0002-5884-0083

REFERENCES

1. W. Huang, Z. Jiang, K. Fukuda, X. Jiao, C. R. McNeill, T. Yokota, T. Someya, *Joule* **2020**, *4*, 128.
2. Y. Li, G. Xu, C. Cui, Y. Li, *Adv. Energy Mater.* **2018**, *8*, 1701791.
3. X. Meng, L. Zhang, Y. Xie, X. Hu, Z. Xing, Z. Huang, C. Liu, L. Tan, W. Zhou, Y. Sun, W. Ma, Y. Chen, *Adv. Mater.* **2019**, *31*, 1903649.
4. H. Li, S. Liu, X. Wu, Q. Qi, H. Zhang, X. Meng, X. Hu, L. Ye, Y. Chen, *Energy Environ. Sci.* **2022**, *15*, 2130.
5. K. Dong, X. Peng, Z. L. Wang, *Adv. Mater.* **2020**, *32*, 1902549.
6. K. Xian, K. Zhou, M. Li, J. Liu, Y. Zhang, T. Zhang, Y. Cui, W. Zhao, C. Yang, J. Hou, Y. Geng, L. Ye, *Chin. J. Chem.* **2022**, *41*, 159.
7. X. Li, R. Xia, K. Yan, J. Ren, H.-L. Yip, C.-Z. Li, H. Chen, *ACS Energy Lett*. **2020**, *5*, 3115.
8. A. Mishra, *Energy Environ. Sci.* **2020**, *13*, 4738.
9. L. Ma, S. Zhang, J. Wang, Y. Xu, J. Hou, *Chem. Commun.* **2020**, *56*, 14337.
10. Y. W. Han, S. J. Jeon, H. S. Lee, H. Park, K. S. Kim, H. W. Lee, D. K. Moon, *Adv. Energy Mater.* **2019**, *9*, 1902065.
11. Q. Liao, B. Li, H. Sun, C. W. Koh, X. Zhang, B. Liu, H. Y. Woo, X. Guo, *Mater. Rep. Energy* **2021**, *1*, 100063.
12. Q. Fan, R. Ma, W. Su, Q. Zhu, Z. Luo, K. Chen, Y. Tang, F. R. Lin, Y. Li, H. Yan, C. Yang, A. K. Y. Jen, W. Ma, *Carbon Energy* **2023**, *5*, e267.
13. Y. Liu, B. Liu, C.-Q. Ma, F. Huang, G. Feng, H. Chen, J. Hou, L. Yan, Q. Wei, Q. Luo, Q. Bao, W. Ma, W. Liu, W. Li, X. Wan, X. Hu, Y. Han, Y. Li, Y. Zhou, Y. Zou, Y. Chen, Y. Li, Y. Chen, Z. Tang, Z. Hu, Z.-G. Zhang, Z. Bo, *Sci. China Chem.* **2021**, *65*, 224.
14. Y. Wang, J. Lee, X. Hou, C. Labanti, J. Yan, E. Mazzolini, A. Parhar, J. Nelson, J. S. Kim, Z. Li, *Adv. Energy Mater.* **2020**, *11*, 2003002.
15. Z. G. Zhang, Y. Li, *Angew. Chem. Int. Ed.* **2021**, *60*, 4422.
16. G. Wang, M. A. Adil, J. Zhang, Z. Wei, *Adv. Mater.* **2019**, *31*, 1805089.
17. Z. Liu, Y. Wu, Q. Zhang, X. Gao, *J. Mater. Chem. A* **2016**, *4*, 17604.
18. L. Ye, H. Ke, Y. Liu, *Trends Chem*. **2021**, *3*, 1074.
19. A. D. de Zerio, C. Müller, *Adv. Energy Mater.* **2018**, *8*, 1702741.
20. Y. Li, Y. Zhang, B. Wu, S. Pang, X. Yuan, C. Duan, F. Huang, Y. Cao, *Solar RRL* **2022**, *6*, 2200073.
21. K. Feng, H. Guo, H. Sun, X. Guo, *Acc. Chem. Res.* **2021**, *54*, 3804.
22. X. Guo, C. Cui, M. Zhang, L. Huo, Y. Huang, J. Hou, Y. Li, *Energy Environ. Sci.* **2012**, *5*, 7943.
23. F. Li, K. G. Yager, N. M. Dawson, Y.-B. Jiang, K. J. Malloy, Y. Qin, *Chem. Mater.* **2014**, *26*, 3747.
24. S. Marina, N. P. Kaufmann, A. Karki, E. Gutierrez-Meza, E. Gutierrez-Fernandez, J. Vollbrecht, E. Solano, B. Walker, J. H. Bannock, J. de Mello, C. Silva, T. Q. Nguyen, D. Cangialosi, N. Stingelin, J. Martin, *Adv. Mater.* **2020**, *32*, 2005241.
25. G. Li, V. Shrotriya, J. Huang, Y. Yao, T. Moriarty, K. Emery, Y. Yang, *Nat. Mater.* **2005**, *4*, 864.
26. Z. Wu, A. Petzold, T. Henze, T. Thurn-Albrecht, R. H. Lohwasser, M. Sommer, M. Thelakkat, *Macromolecules* **2010**, *43*, 4646.
27. K. Zhou, J. Liu, M. Li, X. Yu, R. Xing, Y. Han, *J. Phys. Chem. C* **2015**, *119*, 1729.
28. S. Chatterjee, S. Jinnai, Y. Ie, *J. Mater. Chem. A* **2021**, *9*, 18857.
29. M. Moser, A. Wadsworth, N. Gasparini, I. McCulloch, *Adv. Energy Mater.* **2021**, *11*, 2100056.

26924560, 2024, 2, Downloaded from https://onlinelibrary.wiley.com/doi/10.1002/agt2.466 by Hong Kong Poly University, Wiley Online Library on [22/04/2024]. See the Terms and Conditions (https://onlinelibrary.wiley.com/terms-and-conditions) on Wiley Online Library for rules of use; OA articles are governed by the applicable Creative Commons License

30. X. Yuan, Y. Zhao, D. Xie, L. Pan, X. Liu, C. Duan, F. Huang, Y. Cao, *Joule* **2022**, *6*, 647.
31. J. Xiao, X. Jia, C. Duan, F. Huang, H. L. Yip, Y. Cao, *Adv. Mater.* **2021**, *33*, 2008158.
32. A. T. Kleinschmidt, S. E. Root, D. J. Lipomi, *J. Mater. Chem. A* **2017**, *5*, 11396.
33. D. Han, G.-U. Kim, D. Lee, C. Lim, S. Lee, D. Jeong, S. Cho, C. Lee, B. J. Kim, *Chem. Mater.* **2023**, *35*, 4318.
34. K. Xian, Y. Geng, L. Ye, *Joule* **2022**, *6*, 941.
35. M. Gao, Y. Liu, K. Xian, Z. Peng, K. Zhou, J. Liu, S. Li, F. Xie, W. Zhao, J. Zhang, X. Jiao, L. Ye, *Aggregate* **2022**, *3*, e190.
36. Q. Liang, X. Jiao, Y. Yan, Z. Xie, G. Lu, J. Liu, Y. Han, *Adv. Funct. Mater.* **2019**, *29*, 1807591.
37. X. Xu, G. Zhang, L. Yu, R. Li, Q. Peng, *Adv. Mater.* **2019**, *31*, 1906045.
38. F. Bastianini, G. E. Pérez, A. R. Hobson, S. E. Rogers, A. J. Parnell, M. Grell, A. F. Gutiérrez, A. D. F. Dunbar, *Sol. Energy Mater. Sol. Cells* **2019**, *202*, 110128.
39. Z. Liang, M. Li, Q. Wang, Y. Qin, S. J. Stuard, Z. Peng, Y. Deng, H. Ade, L. Ye, Y. Geng, *Joule* **2020**, *4*, 1278.
40. C. Yang, S. Zhang, J. Ren, M. Gao, P. Bi, L. Ye, J. Hou, *Energy Environ. Sci.* **2020**, *13*, 2864.
41. K. Xian, Y. Liu, J. Liu, J. Yu, Y. Xing, Z. Peng, K. Zhou, M. Gao, W. Zhao, G. Lu, J. Zhang, J. Hou, Y. Geng, L. Ye, *J. Mater. Chem. A* **2022**, *10*, 3418.
42. K. Xian, S. Zhang, Y. Xu, J. Liu, K. Zhou, Z. Peng, M. Li, W. Zhao, Y. Chen, Z. Fei, J. Hou, Y. Geng, L. Ye, *Sci. China Chem.* **2023**, *66*, 202.
43. S. J. Jeon, Y. H. Kim, I. N. Kim, N. G. Yang, J. H. Yun, D. K. Moon, *J. Energy Chem.* **2022**, *65*, 194.
44. X. Xu, Y. Li, Q. Peng, *Adv. Mater.* **2022**, *34*, 2107476.
45. K. Yu, W. Song, Y. Li, Z. Chen, J. Ge, D. Yang, J. Zhang, L. Xie, C. Liu, Z. Ge, *Small Struct*. **2021**, *2*, 2100099.
46. L. Zhu, M. Zhang, J. Xu, C. Li, J. Yan, G. Zhou, W. Zhong, T. Hao, J. Song, X. Xue, Z. Zhou, R. Zeng, H. Zhu, C. C. Chen, R. C. I. MacKenzie, Y. Zou, J. Nelson, Y. Zhang, Y. Sun, F. Liu, *Nat. Mater.* **2022**, *21*, 656.
47. L. Zuo, S. B. Jo, Y. Li, Y. Meng, R. J. Stoddard, Y. Liu, F. Lin, X. Shi, F. Liu, H. W. Hillhouse, D. S. Ginger, H. Chen, A. K. Jen, *Nat. Nanotechnol.* **2022**, *17*, 53.
48. S. Cheng, L. Wang, C. Guo, D. Li, J. Cai, W. Miao, B. Du, P. Wang, D. Liu, T. Wang, *Polymer* **2021**, *236*, 124322.
49. C. He, Y. Pan, Y. Ouyang, Q. Shen, Y. Gao, K. Yan, J. Fang, Y. Chen, C.-Q. Ma, J. Min, C. Zhang, L. Zuo, H. Chen, *Energy Environ. Sci.* **2022**, *15*, 2537.
50. C. Han, J. Wang, S. Zhang, L. Chen, F. Bi, J. Wang, C. Yang, P. Wang, Y. Li, X. Bao, *Adv. Mater.* **2023**, *35*, 2208986.
51. T. Chen, S. Li, Y. Li, Z. Chen, H. Wu, Y. Lin, Y. Gao, M. Wang, G. Ding, J. Min, Z. Ma, H. Zhu, L. Zuo, H. Chen, *Adv. Mater.* **2023**, *35*, 2300400.
52. M. Shi, T. Wang, Y. Wu, R. Sun, W. Wang, J. Guo, Q. Wu, W. Yang, J. Min, *Adv. Energy Mater.* **2020**, *11*, 2002709.
53. P. Cheng, X. Zhan, *Chem. Soc. Rev.* **2016**, *45*, 2544.
54. Y. Yang, W. Chen, L. Dou, W.-H. Chang, H.-S. Duan, B. Bob, G. Li, Y. Yang, *Nat. Photon.* **2015**, *9*, 190.
55. X. Duan, W. Song, J. Qiao, X. Li, Y. Cai, H. Wu, J. Zhang, X. Hao, Z. Tang, Z. Ge, F. Huang, Y. Sun, *Energy Environ. Sci.* **2022**, *15*, 1563.
56. R. Wang, D. Zhang, X. Zhang, J. Yu, *Dyes Pigm.* **2022**, *199*, 110083.
57. W. Song, K. Yu, J. Ge, L. Xie, R. Zhou, R. Peng, X. Zhang, M. Yang, Z. Wei, Z. Ge, *Matter* **2022**, *5*, 1877.
58. S. Chen, L. Hong, M. Dong, W. Deng, L. Shao, Y. Bai, K. Zhang, C. Liu, H. Wu, F. Huang, *Angew. Chem. Int. Ed.* **2023**, *62*, 202213869.
59. S. Zhang, X. Ma, L. Niu, S. Y. Jeong, H. Y. Woo, Z. Zhou, F. Zhang, *Sol. RRL* **2022**, *7*, 2200957.
60. Q. Qi, H. Ke, L. Ye, *Energy Mater*. **2022**, *2*, 35.
61. D. Baran, R. S. Ashraf, D. A. Hanifi, M. Abdelsamie, N. Gasparini, J. A. Rohr, S. Holliday, A. Wadsworth, S. Lockett, M. Neophytou, C. J. Emmott, J. Nelson, C. J. Brabec, A. Amassian, A. Salleo, T. Kirchartz, J. R. Durrant, I. McCulloch, *Nat. Mater.* **2017**, *16*, 363.
62. L. Ye, H. Hu, M. Ghasemi, T. Wang, B. A. Collins, J. H. Kim, K. Jiang, J. H. Carpenter, H. Li, Z. Li, T. McAfee, J. Zhao, X. Chen, J. L. Y. Lai, T. Ma, J. L. Bredas, H. Yan, H. Ade, *Nat. Mater.* **2018**, *17*, 253.
63. C. Yang, R. Yu, C. Liu, H. Li, S. Zhang, J. Hou, *ChemSusChem* **2021**, *14*, 3607.
64. N. Yi, Q. Ai, W. Zhou, L. Huang, L. Zhang, Z. Xing, X. Li, J. Zeng, Y. Chen, *Chem. Mater.* **2019**, *31*, 10211.
65. L. Zhang, N. Yi, W. Zhou, Z. Yu, F. Liu, Y. Chen, *Adv. Sci.* **2019**, *6*, 1900565.
66. D. Leman, M. A. Kelly, S. Ness, S. Engmann, A. Herzing, C. Snyder, H. W. Ro, R. J. Kline, D. M. DeLongchamp, L. J. Richter, *Macromolecules* **2015**, *48*, 383.
67. N. Gasparini, X. Jiao, T. Heumueller, D. Baran, G. J. Matt, S. Fladischer, E. Spiecker, H. Ade, C. J. Brabec, T. Ameri, *Nat. Energy* **2016**, *1*, 16118.
68. W. Gao, Q. An, M. Hao, R. Sun, J. Yuan, F. Zhang, W. Ma, J. Min, C. Yang, *Adv. Funct. Mater.* **2020**, *30*, 1908336.
69. K. Zhou, K. Xian, Q. Qi, M. Gao, Z. Peng, J. Liu, Y. Liu, S. Li, Y. Zhang, Y. Geng, L. Ye, *Adv. Funct. Mater.* **2022**, *32*, 2201781.
70. G. Feng, J. Li, Y. He, W. Zheng, J. Wang, C. Li, Z. Tang, A. Osvet, N. Li, C. J. Brabec, Y. Yi, H. Yan, W. Li, *Joule* **2019**, *3*, 1765.
71. K. Xian, Y. Cui, Y. Xu, T. Zhang, L. Hong, H. Yao, C. An, J. Hou, *J. Phys. Chem. C* **2020**, *124*, 7691.
72. Y. Li, X. Huang, A. R. Mencke, S. K. Kandappa, T. Wang, K. Ding, Z. Q. Jiang, A. Amassian, L. S. Liao, M. E. Thompson, S. R. Forrest, *Proc. Natl. Acad. Sci.* **2023**, *120*, 2301118120.
73. K. Zhou, K. Xian, R. Ma, J. Liu, M. Gao, S. Li, T. Liu, Y. Chen, Y. Geng, L. Ye, *Energy Environ. Sci.* **2023**, *16*, 5052.
74. S. Li, M. Gao, K. Zhou, X. Li, K. Xian, W. Zhao, Y. Chen, C. He, L. Ye, *Adv. Mater.* **2023**, https://doi.org/10.1002/adma.202307278
75. M. Gao, J. Wu, X. Yuan, C. He, H. Jiang, W. Zhao, C. Duan, Y. Chen, Y. Ke, H. Yao, L. Ye, *Energy Environ. Sci.* **2023**, https://doi.org/10.1039/D3EE02354K.

SUPPORTING INFORMATION

Additional supporting information can be found online in the Supporting Information section at the end of this article.

How to cite this article: K. Xian, R. Ma, K. Zhou, J. Liu, M. Gao, W. Zhao, M. Li, Y. Geng, L. Ye, *Aggregate* **2024**, *5*, e466. https://doi.org/10.1002/agt2.466

26924560, 2024, 2, Downloaded from https://onlinelibrary.wiley.com/doi/10.1002/agt2.466 by Hong Kong Poly University, Wiley Online Library on [22/04/2024]. See the Terms and Conditions (https://onlinelibrary.wiley.com/terms-and-conditions) on Wiley Online Library for rules of use; OA articles are governed by the applicable Creative Commons License